ELSEVIER

Vibrational Spectroscopy 23 (2000) 57–69

VIBRATIONAL SPECTROSCOPY

www.elsevier.com/locate/vibspec

Digital iterative deconvolution procedure (DIDP) and its smoothing properties to treat with experimental spectra

Yu.Ya. Efimov *

Institute of Chemical Kinetics and Combustion, 630090 Novosibirsk, Russian Federation

Received 18 March 1999; received in revised form 7 October 1999; accepted 19 October 1999

Abstract

A numerical procedure is proposed for finding a curve that provides a given curve (e.g., experimental spectral contour) in integral convolution with a known function. The experimental curve itself is assumed to be a zero approximation. In order to obtain the required function for the ''i'' iteration, the ''$i-1$'' iteration function is corrected by the difference between the experimental curve and the convolution of the ''$i-1$'' iteration function. The solution obtained is not an oscillating function, as in Fourier self deconvolution, and allows (if necessary) for both the prohibition of a negative value and the limitation on the domain of the required function (break, cut-off). As an example, the statistical frequency distributions of the uncoupled vibrations of liquid water OH-oscillators have been calculated from the Raman spectra from 10 to 200°C. This procedure occurs also to be efficient for smoothing ''noisy'' experimental curves and involves only two parameters: the width of a ''smoothing window'' determining a resolution of the required details of the curve and the number of iterations.

Keywords: Spectral bandshape; Statistical distribution; Inverse problem; Integral convolution; Liquid water; Noise smoothing

1. Introduction

In many areas of spectroscopy, the experimentally obtained curve is, for a number of reasons, the result of integral convolution of the desired spectral distribution with some function which can be often estimated from physical considerations or independent experiments. It is known, for example, that a frequency of the decoupled OH- vibration of a water molecule cannot exceed $\nu_u = 3707\ cm^{-1}$ (unbonded OH-group stretches in vapor) whereas the experimental infrared and Raman spectra in liquid reach 3900 cm^{-1}. Obviously, the intensity observed at $\nu > \nu_u$ does not correspond to any physical states of OH-oscillators. According to the fluctuation concept of hydrogen bonding [1–3], it results from the convolution of the frequency-limited ($\nu \leq \nu_u$) statistical distribution $P(\nu)$ of OH-oscillators in various local surroundings and thus, perturbed by hydrogen bonds of different strength, with an eigen spectral contour of each oscillator (intrinsic lineshape).

Recent advances in computer facilities and new theoretical developments have made it possible to use not only the averaged spectrum characteristics (the peak frequency, integral intensity, half-width,

* Tel.: +7-3832-33-28-54; fax: +7-3832-34-23-50; e-mail: efimov@ns.kinetics.nsc.ru

0924-2031/00/$ - see front matter
PII: S0924-2031(99)00085-5

etc.) but also all details of a band as well as its temperature evolution for studying associated liquids and amorphous solids. It allowed one to formulate a new approach (spectroscopy of statistic contours [1–10]) giving a unique information on the individual characteristics of molecules in a statistic ensemble. Thus, analysis of the temperature dependence of the spectral band shape of liquid water OH-oscillators in IR- [4,5] and Raman spectra [6,7] gave two temperature-independent functions relating to the vibration frequency ν_{OH} of each oscillator to the energy of a hydrogen bond $E(\nu)$, perturbing it and the degeneracy of the realization of such a hydrogen bond, $W(\nu)$. These functions explain the mechanism of energy redistribution in a statistic ensemble of hydrogen bonds with varying temperature, and were used both to describe quantitatively the transformation of spectral contours in the available temperature range, and to propose an approach to calculate a distribution function of H-bond energies and some thermodynamic functions [8–11].

The goal of this paper is to develop a simple and reliable method for obtaining initial data for a similar analysis from experimental spectra. From a mathematical viewpoint, it describes a new algorithm for the solution of the equation of integral convolution. Besides, the paper illustrates the possibility of applying this method for solving another practical problem of experimental data processing, i.e., their smoothing (suppression of statistic noise), with a required degree of resolution of the necessary details of experimental curves.

2. DIDP as the algorithm of solving inverse problem of integral convolution

A standard method for solving the inverse problem of integral convolution

$$S(\nu) = \int_{\nu_1}^{\nu_2} P(\nu')\,\varphi(\nu-\nu')\,\mathrm{d}\nu' \equiv \mathrm{Conv}(P(\nu)), \tag{1}$$

i.e., the determination of $P(\nu) \equiv \mathrm{Deconv}(S(\nu))$ for the known experimental curve $S(\nu)$ and a convolving function $\varphi(\nu)$ in finite limits (ν_1, ν_2), is the inverse Fourier transformation of the result of division of the Fourier transform of $S(\nu)$ by the Fourier transform of $\varphi(\nu)$. Using this technique, in particular, the statistic contours $P(\nu_{OH})$ for isotopically diluted HOD molecules in heavy water have been found from IR-spectra [12]. However, owing to the intrinsic properties of Fourier transformation in its traditional form, the necessity to reproduce the ''break'' of the required $P(\nu)$ at $\nu = \nu_u$, and some other reasons, the resulting solution is oscillating and contains the domains of negative values [13,14]. To eliminate these artefacts correctly in the framework of this method is a nontrivial problem that calls for separate consideration of each concrete case. For example, the interpolation of $P(\nu)$ by a sum of modified Pearson's distributions was used in Ref. [12]. We suggest quite a different method for solving the convolution Eq. (1) and use the analytical expressions for statistic contours $P(\nu,T)$ obtained in Ref. [12] as a model to illustrate our approach.

Let $P(\nu)$ be the required statistic distribution (Fig. 1, curve 1) and $S(\nu)$ (Fig. 1, curve 2) be its convolution (1) with the Lorentzian

$$L(\nu-\nu') = 2H/\left\{\pi\left[H^2 + 4(\nu-\nu')^2\right]\right\}. \tag{2}$$

A given form of a convolving function $\varphi(\nu) = L(\nu)$ corresponds to the homogeneously broadened contour of an individual OH-oscillator involved in the statistic ensemble at its own frequency, ν'; its half-width, $H \equiv \Delta\varphi_{1/2} = 30\ \mathrm{cm}^{-1}$, is estimated from the spectrum of HOD solution in CCl_4. In this non-polar solvent the hydrogen bonds causing the nonequivalence of various OH-oscillators in water, are absent, $P(\nu)$ degenerates into the δ-function nearby ν_u, and the experimental spectral contour $S(\nu)$ must reduce to $\varphi(\nu)$.

Our aim is to obtain curve 1 from curve 2 (Fig. 1) for the known $\varphi(\nu)$. As zero approximation, we take $P^0(\nu) = S(\nu)$, i.e., curve 2 (which is already the result of convolution of the required $P(\nu)$ with $L(\nu)$) and convolve it with $L(\nu)$ again (squares 3 in Fig. 1a). Let us calculate the incompatibility (misfit) function $\delta^1(\nu)$ as the difference between ''experimental'' $S(\nu)$ (curve 2), and the obtained curve 3. As the first approximation for $P(\nu)$, we assume that $P^1(\nu) = P^0(\nu) + \delta^1(\nu)$ (dots 1 in Fig. 1a). The convolution of this curve with $L(\nu)$ (circles 2 in

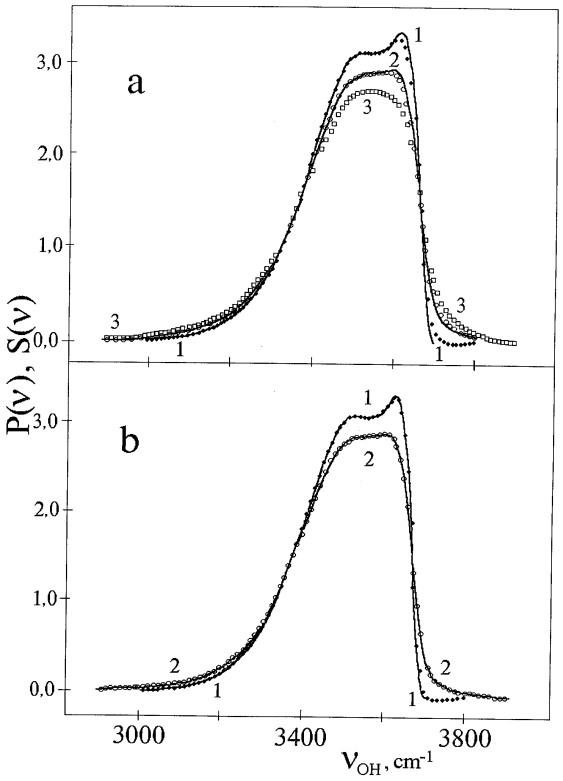

Fig. 1. DIDP in its simplest variant (Eqs. (3) and (4)). Solid line 1: statistical contour P(ν) of OH vibrations of water molecules in liquid at 100°C calculated from IR-spectra of diluted HOD solution in D_2O [12], curve 2: its convolution, $S(\nu)$, with Lorentzian contour $\varphi(\nu)$ of half-width $H = 30$ cm^{-1} (the model of experimental spectrum, see Eq. (1)). (a) Result of first iteration (dots 1 and circles 2 for curves 1 and 2, respectively). Squares 3: convolution of curve 2 with Lorentzian contour; (b) Result of third iteration (see Eq. (3) for $i = 3$).

Fig. 1a) shows that already first iteration describes well the ''experiment'', $S(\nu)$, starting from $P^1(\nu)$. Fig. 1b depicts the result of third iteration (dots and circles) compared to models $P(\nu)$ and $S(\nu)$, respectively.

In the general form our procedure in its simplest variant is as follows

$$P^i(\nu) = P^{i-1}(\nu) + \delta^i(\nu)$$
$$\delta^i(\nu) = S(\nu) - \mathrm{Conv}^{i-1}(\nu) \qquad (3)$$
$$\mathrm{Conv}^i(\nu) = \int_{\nu_1}^{\nu_2} P^i(\nu')^* \varphi(\nu - \nu')\mathrm{d}\nu'$$

for given initial conditions

$$P^0(\nu) = S(\nu)$$
$$\mathrm{Conv}^0(\nu) = \int_{\nu_1}^{\nu_2} P^0(\nu')\varphi(\nu - \nu')\mathrm{d}\nu' \qquad (4)$$

All calculations have been performed by a set of discrete points from 2900 to 3900 by 10 cm^{-1} with no extrapolation or cut-off, summation was used instead of integration.

It can be shown that Eqs. (3) and (4) realize the iteration solution of inhomogeneous integral Fredholm equation of second type by a formal Neuman series. A rigorous foundation of procedure convergence is beyond the framework of this paper. For brief remarks and references see Appendix A.

In the above real example, the convolving function $\varphi(\nu)$ estimated from the independent experiment, appeared to be much more narrow than the statistic distribution, $P(\nu)$. Three to five iterations are quite sufficient in this case to find the solution differing from the initial (model) curve within the level of experimental errors, characteristic for infrared measurements. Fig. 2 shows the case where the $P(\nu)$ and $\varphi(\nu)$ widths are comparable in their values. In this case, tens of iterations are necessary to reach similar agreement of the solution derived (dots and circles) with the known one (solid lines). Nevertheless, the procedure allows one to restore the curve of statistic distribution 1 with two well pronounced maxima from the Gauss-like ''experimental'' curve 2 with no visible bimodality.

Fig. 2,a shows results obtained by the same simplest scheme (Eq. (3)) as in Fig. 1. In both cases near 3700 cm^{-1}, we observe a small region of negative values, similar to the solution from Fourier self deconvolution, which is followed by the region of positive values although $P(\nu)$ at $\nu > \nu_u$ is sure to be a zero. A simple way to avoid this defect is the introduction of an artificial limitation on each iteration

$$P^i(\nu) = P^{i-1}(\nu) + \delta^i(\nu), \text{ if } P^i(\nu) \geq 0 \qquad (5a)$$
$$P^i(\nu) = 0, \text{ if } P^i(\nu) < 0 \text{ or } \nu > \nu_u \qquad (5b)$$

Two different limitations in Eq. (5b) can be used separately if, for example, it is necessary to provide the non-negativity of the required $P(\nu)$ with no

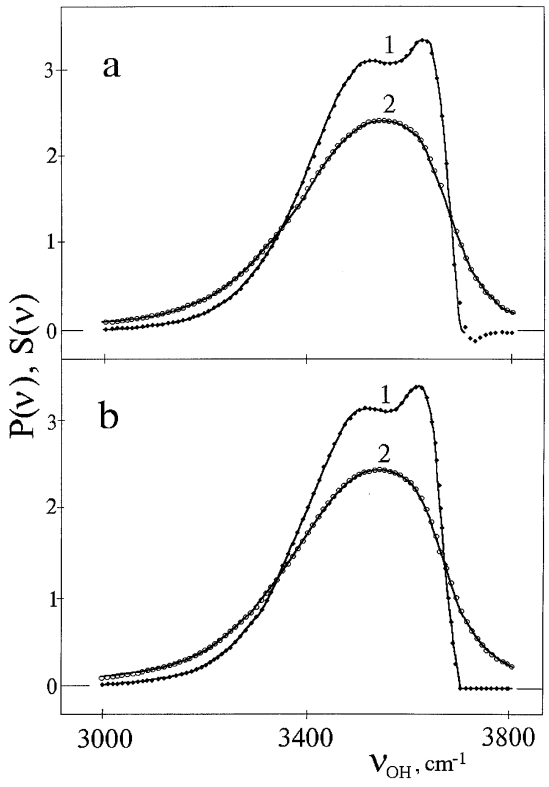

Fig. 2. Deconvolution of spectral contour in the case of strong homogeneous broadening. Solid line 1: the same as in Fig. 1, curve 2: its convolution (1) with Lorentzian contour with a half-width of 100 cm^{-1}. Dots 1 and circles 2: reconstructed $P(\nu)$ and $S(\nu)$, respectively. Result of 30th iteration. (a) Procedure in the simplest variant (Eqs. (3) and (4)); (b) DIDP with prohibition of the negative values of $P(\nu)$ and condition $P(\nu)=0$ for all $\nu > \nu_u$ (Eqs. (3) and (4) with limitation 5).

limitation of its domain of definition or, on the contrary, to set the domain of $P(\nu)$ without demands of its sign constancy. These limitations providing the positively defined solution for $P(\nu)$ effect neither the convergence of the procedure, nor the computation time, which is about 1 s per 10 iterations by IBM PC with the 486 processor.

Fig. 2b shows that such a modification of DIDP allows one to obtain the solution corresponding to the physical meaning (dots 1). In this case, its proving convolution (circles 2) coincides with the ''experimental'' curve 2 no worse than in Fig. 2a both visually and according to the residual sum of squares. This illustrates the known fact that the inverse problem of integral convolution within finite limits at the finite point set has many solutions. Section 3 demonstrates that the oscillating solutions are also possible among of them, particularly if a non-smoothed (complicated by statistic noise) curve is used as $S(\nu)$.

It is interesting to note that if a non-negative solution does not exist (for example, if the intrinsic linewidth, H, was chosen too large for the deconvolution procedure), the family of consequent $P^i(\nu)$ distributions does not diverge. It converges to a curve which does not fit the ''experiment'', $S(\nu)$, after the convolution, indeed, but provides the minimal possible residual sum of squares between $S(\nu)$ and $S^i(\nu)$.

3. Spectrum deconvolution in the presence of statistic noise

In Section 2 we used the analytically determined, i.e., ideally smooth, initial curves. Any real spectrum is noisy, i.e., most points deviate from the ''ideally smooth'' curve. In this case, the above mentioned iteration procedure of finding $P(\nu)$ increases repeatedly such deviations (solid lines in Fig. 3b,c) by adding intensity to $P^i(\nu)$ at frequencies where the $S(\nu)$ points lie above the ''ideally smooth'' curve and by subtracting intensity from $P^i(\nu)$ for the points lying below this curve. Thus, the solution, $P^i(\nu)$, diverges in this case, and the level of ''noise'' will exceed the spectrum magnitude after few tens of iterations. However, since the incompatibility function, $\delta^i(\nu)$, which governs the iteration process, is counted from the ''noisy'' curve, the convolution of this solution with the Lorentzian contour, $\varphi(\nu)$, is still in agreement with the model of experiment (circles and solid lines in Fig. 3a) as in the case of smooth $S(\nu)$ (Figs. 1 and 2). This testifies to the fact that the oscillating curves are also the solutions of the inverse problem. Such behavior is observed both with (Fig. 3b) and without (Fig. 3c) limitations (5) which leads to different solutions, indeed. It is concluded then that before solving the inverse problem it is necessary to smooth carefully the experimental curves to obtain the physically comprehended solu-

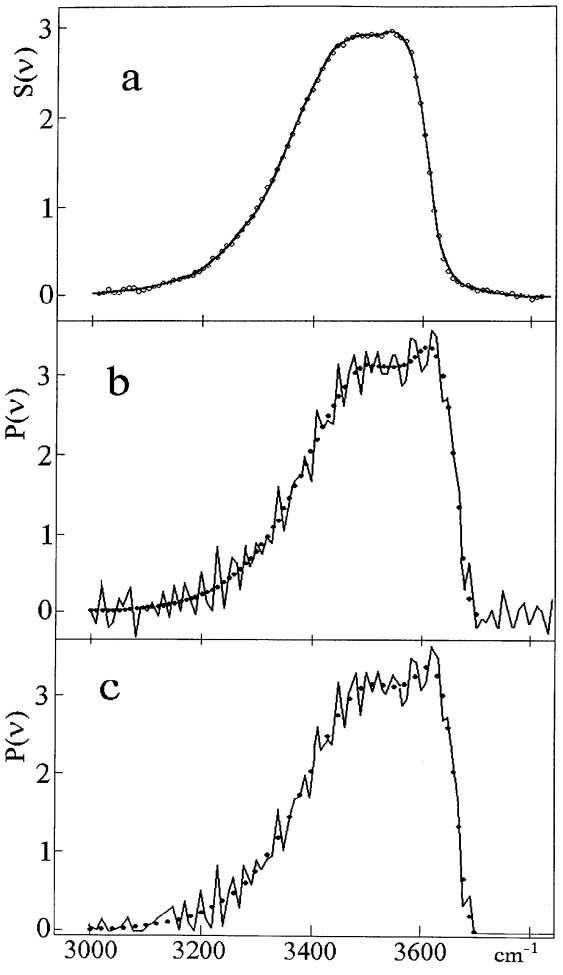

Fig. 3. DIDP in the presence of statistic noise. (a) Circles: experimental spectrum model (curve 2 in Fig. 1 with addition of random noise of amplitude up to 1% of the peak intensity); solid line: the result of the convolution of calculated $P^i(\nu)$ (oscillating curve in b) with a Lorentzian (half-width of 30 cm^{-1}). (b) Dots: a given initial distribution of $P(\nu)$ (the same as curve 1 in Fig. 1), oscillating curve: the result of 30 iterations by Eqs. (3) and (4) without limitation (5b). (c) the same as in b but using limitation (5b).

tions from the set of possible ones. Fourier self-deconvolution is free of this complication.

We can, however, modify slightly the DIDP algorithm involving its internal smoothing facilities. Thus, if the calculated $\delta^i(\nu)$ value is added to $P^{i-1}(\nu)$ not only at a given frequency ν, but also at the neighbouring ones by distributing it in decreasing order with respect to its closeness to this frequency (e.g., according to the Lorentzian or Gaussian distribution law $\chi(\nu-\nu')$)

$$P^i(\nu) = P^{i-1}(\nu) + \int_{\nu_1}^{\nu_2} \delta^i(\nu')^* \, \chi(\nu-\nu')\,\mathrm{d}\nu' \tag{6}$$

then, owing to the mutual compensation of contributions of the points ''falling'' above and below $S(\nu)$, we can block up a progressing ''noise'' in $P(\nu)$ (Figs. 4 and 5). A half-width of such a smoothing distribution, $\Delta\chi_{1/2}$, should be large enough to pre-

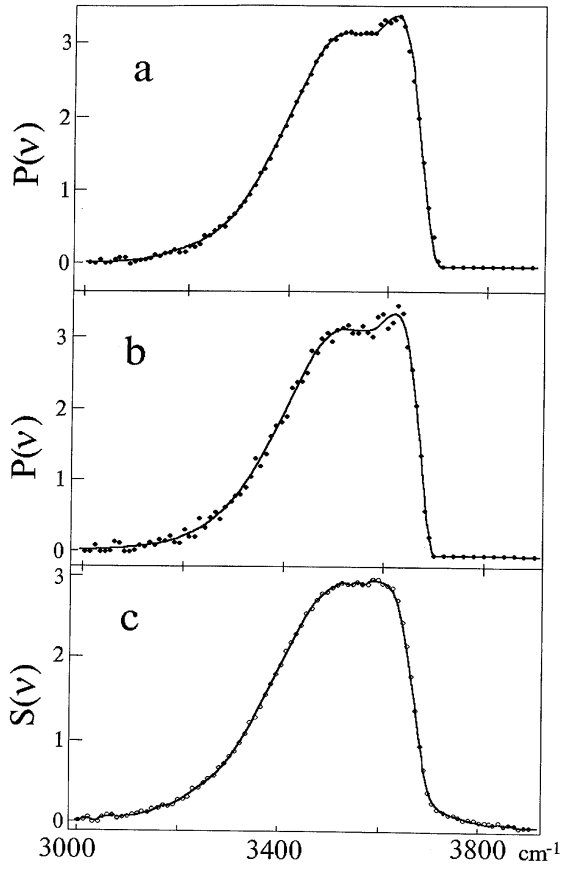

Fig. 4. The result of the deconvolution of a noisy spectrum (circles in Fig. 3a) with internal suppression of noise (Eq. (6) instead of Eq. (5a) after three (a) and 50 (b) iterations. $\Delta\chi_{1/2} = 20$ cm^{-1}. Solid line: initial $P(\nu)$, dots: its reconstruction, $P^i(\nu)$. (c) Solid line: result of convolution of the solution, $P^i(\nu)$ (dots in b), with $\varphi(\nu)$, cirlces: a model of noisy experimental curve (Fig. 3a).

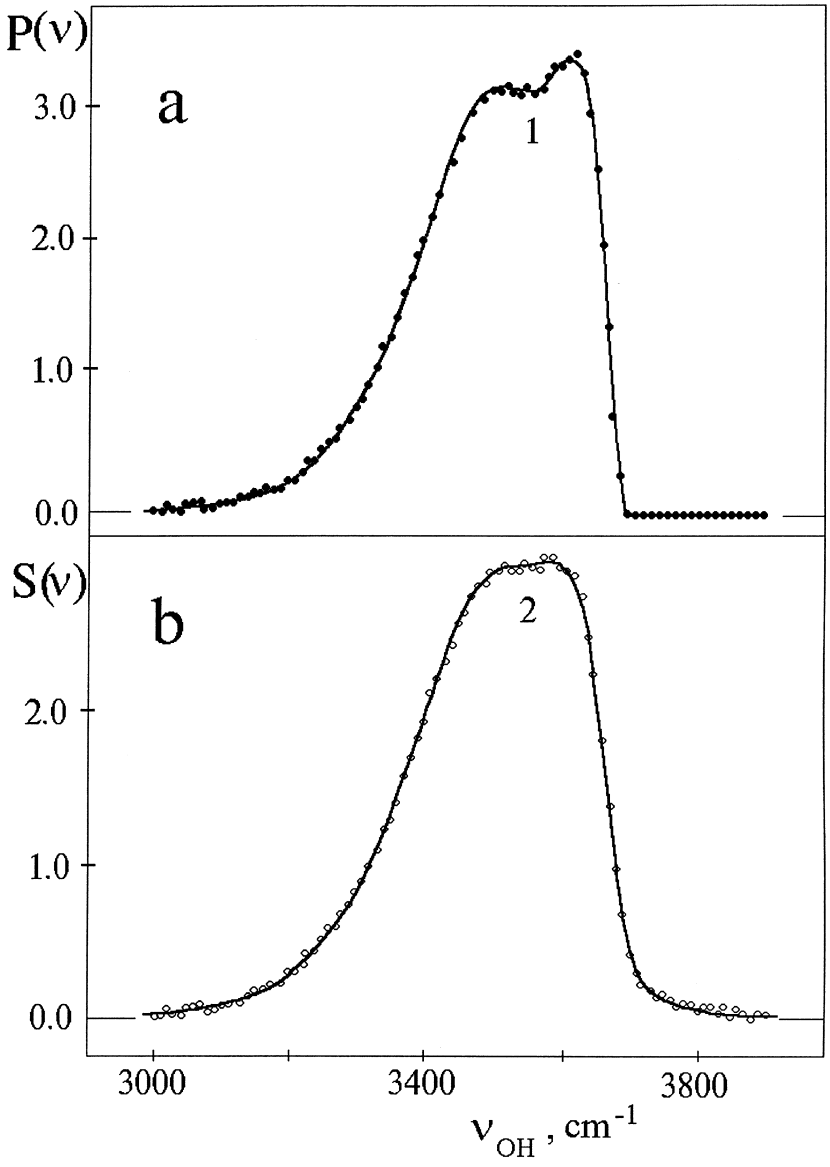

Fig. 5. (a and b): the same as in Fig. 4b,c but for $\Delta\chi_{1/2} = 100\ \mathrm{cm}^{-1}$.

vent an increase in noise amplitude but not to hamper the restoration of substantial details of the spectrum and to require a great number of iterations. The latter is important because the computation time in this variant of DIDP enlarges about an order of magnitude per 1 iteration as compared to Eqs. (3) and (4) or Eqs. (5a) and (5b).

As an example, Fig. 4a,b show that $\chi(\nu)$ with $H = 20\ \mathrm{cm}^{-1}$ does not provide efficient noise suppression. Three iterations are enough to resolve main features of $P(\nu)$, but the noise level grows up approximately twice (Fig. 4a). As the number of iterations increases, the noise amplitude continues to increase (Fig. 4b). It is interesting that the convolu-

tion of the obtained $P(\nu)$ with $\varphi(\nu)$ tends in this case to the noisy $S(\nu)$ (Fig. 4c, solid line and circles, respectively).

When we take the Lorentzian with half-width $H = 100\ \mathrm{cm}^{-1}$ as $\chi(\nu)$, an increase in noise amplitude is fully suppressed (Fig. 5a). However, the

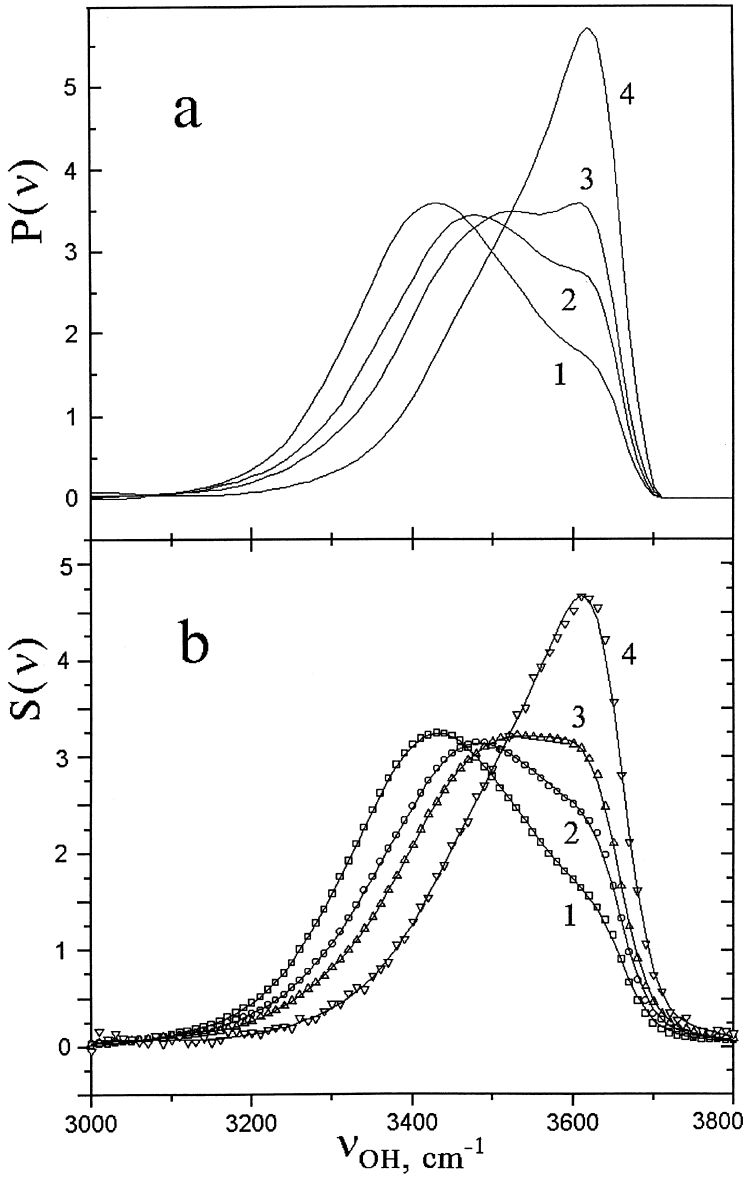

Fig. 6. (a) Statistic $P(\nu)$ distributions of the frequencies of OH-group vibrations in liquid water molecules at 10°C (1), 50°C (2), 90°C (3) and 200°C (4) calculated from experimental spectra [15,16]. Convolving function: Lorentzian with $H = 30\ \mathrm{cm}^{-1}$. Algorithm with limitations (5) is used, $\nu_u = 3707\ \mathrm{cm}^{-1}$. (b) circles: experimental spectra of an isotropic component of the Raman spectra of diluted H_2O solution in heavy water D_2O [15] (10–90°C) and [16] (200°C) normalized by area to unity. Solid lines: a checking convolution of determined $P^i(\nu)$ (a) with Lorentzian of half-width $H = 30\ \mathrm{cm}^{-1}$.

number of necessary iterations amounts to several tens. The misfit function, $\delta^i(\nu)$, decreases monotonously with the iteration number, i, so the solution in this case is converging in respect to both $P(\nu)$ and $S(\nu)$.

In general, we couldn't give at present a strict rule for determination of H value for $\chi(\nu)$. It is a subject for more detailed investigation, including the separation of H values leading to convergence or divergence in $P(\nu)$ solution. The best way to avoid

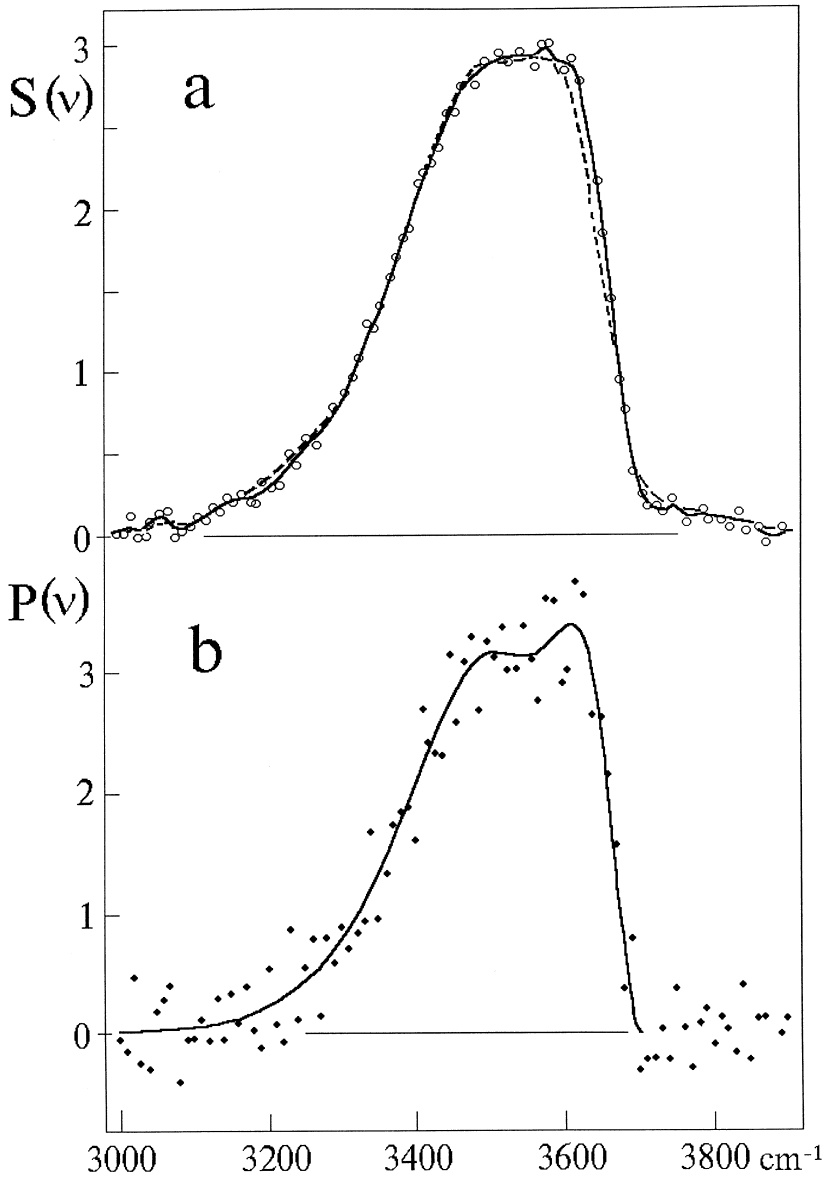

Fig. 7. Smoothing of model S(ν) curve with random noise up to $\pm 3\%$ of peak intensity (circles) by the simplest algorithm (Eqs. (3) and (4)), $H = 30\ \mathrm{cm}^{-1}$. (a) the number of iterations $i = 1$ (dashed line) and 5 (solid line); (b) dots: $P^i(\nu)$ at $i = 5$, solid line: $P(\nu)$ (curve 1 in Fig. 1a).

this problem is to smooth experimental spectra, when possible, and use less complicated variant of DIDP.

It is interesting to note that the convolution checking the solution obtained for $H = 100\ cm^{-1}$ (Fig. 5b, solid line) almost coincides in this case with the initial smooth $S(\nu)$ depicted by curve 2 in Fig. 1 rather than with the ''experimental'' noisy $S(\nu)$ (Fig. 5b, circles) as it was in Fig. 4c. This illustrates the known smoothing property of convolution procedure which will be further used to construct a simple and efficient smoothing algorithm.

As the practical application of the DIDP method, we calculated the statistical distributions of the frequencies of liquid water OH-oscillators from Raman spectra (Fig. 6) in addition to similar distributions derived earlier from IR spectra [12]. The results

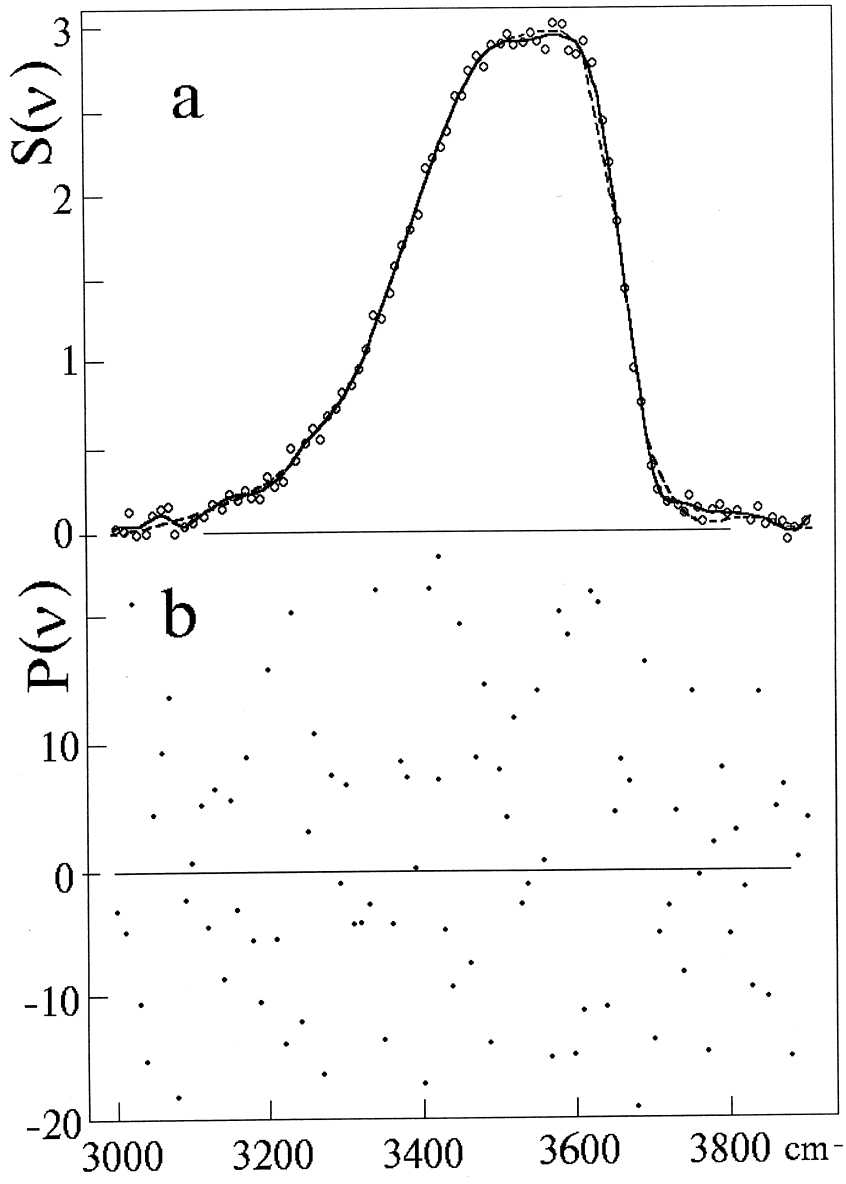

Fig. 8. The same as in Fig. 7 at $H = 100\ cm^{-1}$, $i = 10$ (dashed line) and $i = 250$ (solid line). Points in b: $P^i(\nu)$ at $i = 250$.

obtained are very close, although there is a sharp difference between two sets of initial spectra caused by the different dependence of spectral intensity on hydrogen bond strength in these two experimental methods. This fact verifies the validity of the statistical contours calculated.

4. DIDP as a smoothing algorithm with a controlled degree of resolution of details

There are many methods for smoothing the curves with noise, e.g., polynomial approximation by the least-squares fit and smoothing splines, the methods

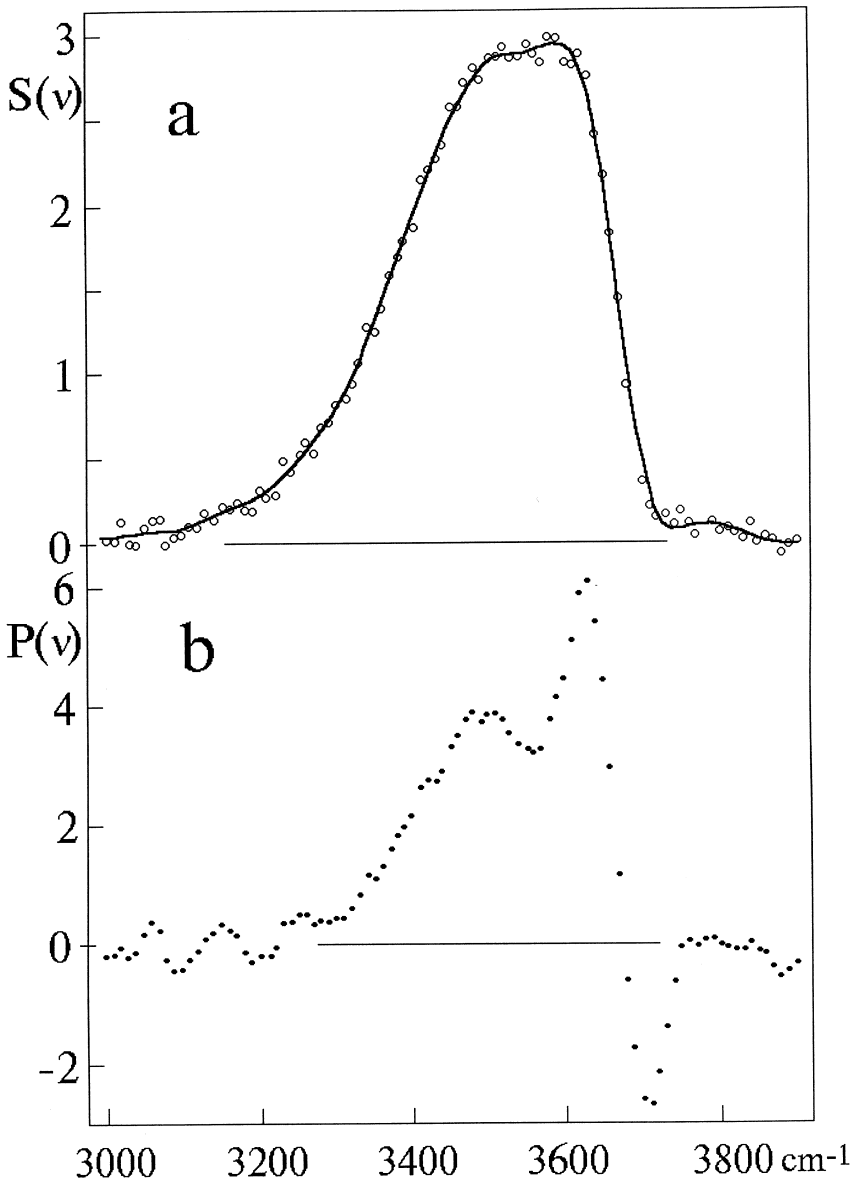

Fig. 9. The same as in Figs. 7 and 8 but using the algorithm for self-suppressing noise in $P^i(\nu)$ (Eq. (6) at $\Delta\chi_{1/2} = 50\ \mathrm{cm}^{-1}$). $H = 100\ \mathrm{cm}^{-1}$, $i = 50$; (a) circles: initial curve with noise, solid line: $S^i(\nu)$ at $i = 50$. (b) $P^i(\nu)$ at $i = 50$.

of spectral filtration based on Fourier transformation with the truncation of the highest harmonics. Our method has so much in common with the latter, because it transforms the entire curve (not the fragments with their sewing as, e.g., when using smoothing splines), employs a direct and inverse transformation (in our case these are convolution and deconvolution) and allows one to regulate a smoothing scale (in our case by varying the half-width of a convolving distribution $\varphi(\nu)$ and the number of iterations). The difference is in the fact that the ''auxiliary'' function is not sine (or cosine) but just

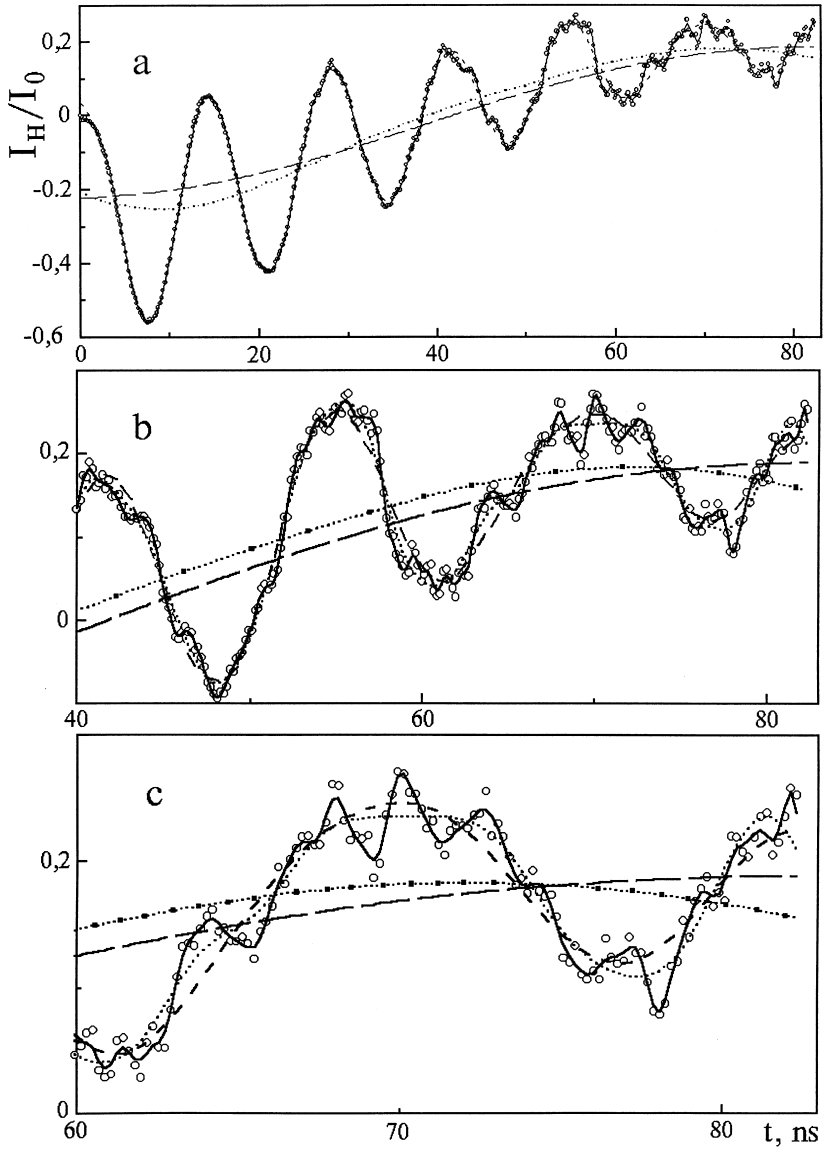

Fig. 10. Variants of smoothing of a real set of 445 experimental points [17] (circles) by the simplest algorithm (Eqs. (3) and (4)). As a convolving function $\varphi(\nu)$, we take the Gaussian with half-width $\Delta\varphi_{1/2} = 5$ of experimental points (solid line), 20 points (dotted line), 50 points (short-dash line), 200 points (dash-and-dotted lines) and 500 points (long-dash line). The number of iterations $i = 10$ for all cases except $\Delta\varphi_{1/2} = 50$ points (short-dash line) where $i = 30$. (a) the entire smoothed curve; (b and c) its fragments on an enlarged scale.

an arbitrary function normalized by area to unity including triangle, trapezoid or rectangle which allows one to choose the most effective variant for a concrete smoothing signal. In addition, the main smoothing parameter (the half-width of contour $\varphi(\nu)$) has an obvious physical meaning of the width of ''filtration window'' in the direct rather than inverse space. (In Fourier smoothing procedure this role is played by a cut-off in the reverse Fourier transform).

The algorithm idea is based on the smoothing properties of convolution transformation and is as follows. Let $S(\nu)$ be an experimental curve to be smoothed. As in Section 2, it is subjected to iteration (formulas (3)–(4)). However, compared to the problem of deconvolution search, the main attention is paid not to $P(\nu)$ but to $S(\nu)$. The form and half-width of the convolving function $\varphi(\nu)$ are not related to any real process (the intrinsic spectral contour of an individual oscillator, apparatus function, etc.) and can be chosen with respect to the required resolution of the smoothed curve peculiarities. Our calculations demonstrate that when the number of iterations, i, tends to infinity, $S^i(\nu)$ converges to the initial (noisy) curve. Stopping the process of deconvolution–convolution for various i, we obtain the different smooth $S^i(\nu)$ curves differing in the degree of closeness to the initial (noisy) $S(\nu)$. In this case, the wider is the convolving function $\varphi(\nu)$, the greater is the degree of smoothing after first few iterations (the analog of ''truncation'' of high frequencies in the methods of spectral filtration) and the greater is the number of iterations necessary to reach the resolution of ''high-frequency'' features if it is assumed that they have a physical meaning and do not result from random fluctuations. Thus, the number of i iterations so as $\Delta\varphi_{1/2}$ becomes the main parameter of smoothing.

As is expected, when using the simplest variant of DIDP algorithm according to formulas (3)–(4), the

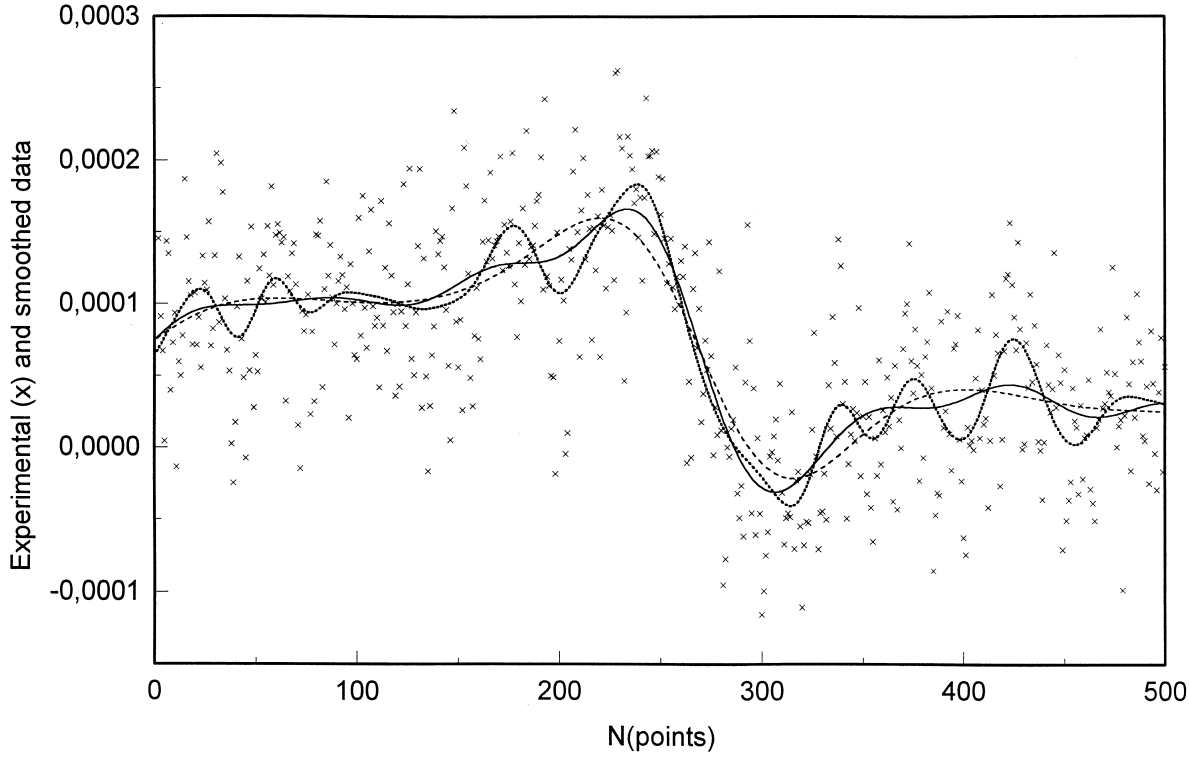

Fig. 11. Variants of smoothing of highly noisy data for 505 experimental points [17]. $\Delta\varphi_{1/2} = 31$ points, 71 and 101 points, respectively. Results of 10 iterations.

noise on the $P^i(\nu)$ function increases constantly with increasing number of iterations (Fig. 7b) bringing this function seemingly close to the spectrum of white noise (Fig. 8b). However, as has been mentioned, this function has an auxiliary character in a smoothing algorithm and of importance is only the fact that its convolution with $\varphi(\nu)$ gives further a smooth $S(\nu)$ (Fig. 7a and Fig. 8a).

Internal self-suppression of noise (formula 6) when smoothing $S(\nu)$ (Fig. 9a) has no obvious advantages over the simplest DIDP algorithm although the $P^i(\nu)$ form remains in this case (Fig. 9b) less senseless than that in Fig. 8b. In particular, the domain of negative values at $\nu \sim \nu_u$ implies that the problem of deconvolution of a given spectral contour by such a wide Lorentzian (a half-width of $\varphi(\nu)$, $H = 100\ \mathrm{cm}^{-1}$ was used) has no positive solution. It was confirmed by the failure to obtain such a non-negative $P(\nu)$ (by imposing limitations (5b)) which could describe satisfactorily $S(\nu)$ after the convolution with $\varphi(\nu)$.

Fig. 10 shows the peculiarities of our method when smoothing the curve with the form differing extremely from the above spectral contours. Particularly, it is alternating and is of a pronounced oscillating nature, possibly, with several frequencies. Varying the width of a convolving function, we can obtain various smooth curves to describe both the high-frequency (solid line) and low-frequency (short-dash line) oscillations and to average them completely (long-dash line).

Fig. 11 illustrates potentialities of the procedure in smoothing a set of experimental data with a very high level of noise. The given curves correspond to three different widths of a ''smoothing window''. As this width decreases further, the smoothed curves describe an increasing number of local minima and maxima in distribution of experimental points, and at $\Delta\varphi_{1/2} = 1–3$ they cross all points after several iterations without increasing noise amplitude.

Acknowledgements

The author is grateful to Profs. A.B. Doktorov, Yu.N. Molin, and Yu.I. Naberukhin for helpful discussions and remarks. This work was supported in part by grant 3H-236-98 of the Ministry of Higher Education of Russian Federation.

Appendix A

Eq. (1) is a linear integral equation of first type with a symmetric core $K_1(\nu,\nu') = \varphi(\nu - \nu')$. It is readily transformed into inhomogeneous integral Fredholm equation of second type

$$P(\nu) = S(\nu) + \int_{\nu_1}^{\nu_2} K_2(\nu,\nu')\,P(\nu')\,\mathrm{d}\nu' \qquad (7)$$

(see [18]), with the core

$$K_2(\nu,\nu') = \delta(\nu - \nu') - \varphi(\nu - \nu'). \qquad (8)$$

Here, $\delta(\nu - \nu')$ is the Dirac delta-function (not to be confused with our misfit function $\delta^i(\nu)$ in Eqs. (3), (5a) and (5b) and in the text).

Successive approximations

$$P^i(\nu) = S(\nu) + \int_{\nu_1}^{\nu_2} K_2(\nu,\nu')\,P^{i-1}(\nu')\,\mathrm{d}\nu', \qquad (9)$$

numerically realized by Eqs. (3) and (4), give the Newman series converging under certain conditions for $P(\nu)$ solution.

References

[1] Y.Y. Efimov, Y.I. Naberukhin, Mol. Phys. 30 (1975) 1621.
[2] Y.Y. Efimov, Y.I. Naberukhin, Mol. Phys. 33 (1977) 759.
[3] Y.Y. Efimov, Y.I. Naberukhin, Mol. Phys. 36 (1978) 973.
[4] A.P. Zhukovskii, J. Struct. Chem. (Russian) 17 (1976) 931.
[5] H. Palamarev, G. Georgiev, J. Mol. Struct. 378 (1996) 237.
[6] Y.Y. Efimov, Y.I. Naberukhin, J. Struct. Chem. (Russian) 21 (1980) 95.
[7] D.E. Hare, C.M. Sorensen, J. Chem. Phys. 93 (1990) 6954.
[8] Y.Y. Efimov, Y.I. Naberukhin, Faraday Discuss. Chem. Soc. 85 (1988) 117.
[9] Y.Y. Efimov, J. Mol. Struct. 141 (1986) 419.
[10] Y.Y. Efimov, J. Mol. Struct. 237 (1990) 93.
[11] A.P. Zhukovskii, N.V. Rovnov, J. Appl. Spectr. (Russian) 41 (1984) 229.
[12] H. Palamarev, G. Georgiev, Vib. Spectrosc. 7 (1994) 255.
[13] V. Zhelyaskov, G. Georgiev, Zh. Nickolov, M. Miteva, Mol. Phys. 64 (1988) 1133.
[14] V. Zhelyaskov, G. Georgiev, Zh. Nickolov, J. Raman Spectrosc. 19 (1988) 405.
[15] J.R. Scherer, M.K. Go, S. Kint, J. Phys. Chem. 78 (1974) 1304.
[16] C.I. Ratcliffe, D.E. Irish, J. Phys. Chem. 86 (1982) 4897.
[17] Yu.N. Molin (private communication).
[18] G.A. Korn, T.M. Korn, Mathematical Handbook for Scientists and Engineers, McGraw-Hill, New York, 1968.